AAS 19-091

GUIDANCE AND NAVIGATION DESIGN TRADES FOR THE LUNAR PALLET LANDER

Evan Anzalone,[*] Ellen Braden,[†]
Naeem Ahmad, Jason Everett, and Kyle Miller[‡]

This paper provides an overview of a series of design trades in support of the NASA Lunar Pallet Lander (LPL) project. The vehicle is being designed to enable a high mass landing capability on the Lunar surface with a high precision. In order to provide clear requirements definition and preliminary design, the Guidance and Navigation Teams are assessing areas such as algorithm development, sensor architectures, and system-level sensitivities. These trades are enabled by the detailed six degree of freedom analysis tools. This mature simulation with the capability for closed- and open-loop simulation modes allows for high fidelity modeling and understanding of the system under design. The results show the feasibility and performance of the current vehicle to meet high accuracy landing requirements.

INTRODUCTION

To support the development of the NASA large payload Lunar Pallet Lander (LPL), a series of guidance and navigation trades provide insight into the sub-system design and requirements to support high precision landing on the lunar surface. This research presents a detailed overview of the design trades and options to support the vehicle's preliminary design. The core assumptions on the mission scenario, vehicle inputs, and high-level vehicle requirements provide constraints on the guidance and navigation performance needed for this mission scenario.

In order to support high precision landing, accurate knowledge of the vehicle's state is needed to enable the use of advanced guidance algorithms during the descent phase. To meet these system requirements, an expanded sensor suite is considered including: Terrain Relative Navigation (TRN), Altimeters, Velocimeters, Inertial Measurements Units (IMU), and Star Trackers. The trades define the sensor requirements and provide insight into balancing performance across sensors. For example, while exact TRN algorithms are not provided in detail, the results define the requirements at a system level in terms of position measurement accuracy, while still considering accurate error dynamics and noise. The Generalized Lander Simulation in Simulink (GLASS) was used with high fidelity sensor models in order to trade individual sensor accuracy via Monte Carlo and Covariance-based analysis. Additionally, the research provides insight into system sensitivities to star tracker outage altitude, TRN altitude requirements, as well as allowable sensor misalignments.

With high accuracy state knowledge, it is possible to take advantage of advanced closed-loop guidance algorithms to ensure the vehicle can meet landing position and velocity requirements. Several approaches to landing guidance are implemented in the GLASS simulation. The team implemented a range of approaches incorporating elements of numerical and analytical optimal guidance. These results capture the performance of the individual algorithms and provide information pertaining to implementation effects and considerations

[*] Guidance and Navigation Team Lead, EV42, NASA/MSFC, Huntsville, AL 35801
[†] Aerospace Engineer, EG511, NASA/JSC, 2101 NASA Parkway, Houston, TX, 77058
[‡] Aerospace Engineer, EV42, NASA/MSFC, Huntsville, AL 35801

in the use of each. These results provide insight into the requirements development and algorithm and sensor selection trades that support high precision landing from a Guidance and Navigation perspective.

Mission Description

The focus of the Lunar Pallet Lander is to demonstrate a high accuracy, large payload lunar landing vehicle. As such, the system level requirements focus on maximizing the mass delivered to the surface and also landing site accuracy. This latter requirement is currently defined as landing within a 100 meter radius of the desired location. In addition to this, the vehicle must also land successfully, with no damage to the lander or payload. This translates to altitude knowledge prior to landing for commanding engine shutdown to ensure a soft landing, as well as landing velocity requirements in the lateral direction as well as attitude requirements to ensure post-landing communication with Earth and payload exit. The proposed Concept of Operations for the mission is given in Figure 1 below. The payload will be placed into a translunar trajectory by the selected launch vehicle. It is assumed that the lander is the primary payload on a dedicated mission. Upon separation from the vehicle's upper stage, the payload will power on and enter into a checkout phase to ensure system operability and prepare for lunar descent. During this phase, the payload will communicate with Deep Space Network (DSN) tracking stations for time, position, and velocity updates. The final tracking pass will be scheduled in order to provide a final state update prior to powered descent. The first stage of powered descent will be performed by a solid rocket motor to reduce the lander's velocity. Upon motor burnout and ejection, the lander will then use its liquid engines for final descent and approach to the desired landing site.

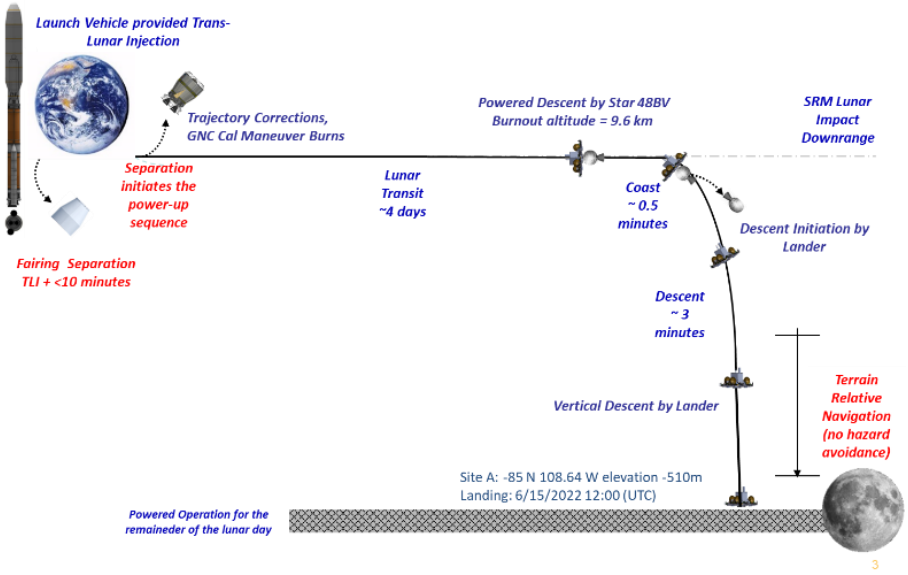

Figure 1: Mission Concept of Operations

These mission level requirements are used to define the design and operation of the guidance, navigation, and control system. The focus on this research is the selection of the necessary navigation sensors, and flight algorithms needed to achieve the desired landing requirements. The following table summarizes the high-level requirements driving the guidance and navigation design. In order to achieve these, the lander is utilizing a closed loop guidance algorithm to enable high-efficiency maximal mass to the surface while taking advantage of as-flown dispersions to enable a high fidelity landing. To support these landing algorithms, the navigation system must provide an accurate solution. In order to do this, the vehicle utilizes TRN[1], providing absolute state measurements during descent, and altimetry and velocimetry measurements via the Navigation Doppler LIDAR (NDL)[2] to ensure high accuracy velocity knowledge during final descent. The baseline system design and performance are described in detail in a companion paper[3].The following sections provide detailed descriptions of the subsystem designs.

GUIDANCE ALGORITHM DEVELOMPENT

The Guidance system's function is to command attitude, angular rates and engine thrust (applicable only to the liquid engines) so that the guidance targets are achieved without violating design constraints. The Guidance system depends on navigated inertial position, inertial velocity, attitude, and the current time from the Navigation subsystem. The Mission Manager supplies the Guidance system with inputs for event notifications and engine status. The remaining inputs to the Guidance algorithms are mission-dependent data and constants, which are loaded onto LPL in the form of loadable parameters. Outputs from the Guidance system passed to the Control system include the estimate of liquid propellant remaining, as well as commanded attitude and angular velocity. Additionally, the Guidance system outputs the recommended shutdown command to the liquid engines. Another study[4] provides a detailed summary of Powered Descent Algorithms.

The Guidance system is divided into four main areas: Coast Guidance, Braking Guidance, Powered Descent Guidance, and Vertical Descent Guidance. Coast Guidance is firstly used in the Pre-SRM mission phase, which starts at the time of separation from the ELV upper stage and ends at the beginning of Solid Rocket Motor (SRM) ignition. There are also two Post-SRM Coast Guidance phases: one between SRM shutdown and ignition of the liquid engines, and one right before the Vertical Decent phase. Braking Guidance occurs during the SRM burn. Powered Descent Guidance, using pulsed liquid engines, occurs after the Post-SRM Coast and lasts until the LPL has achieved a specified target above the landing site. Lastly, the Vertical Descent phase begins at the specified target above the lunar surface and lasts until the LPL touches down at the target site. During each phase, an appropriate guidance scheme is used, with some phases containing multiple guidance schemes to be used for trade studies. Table 1 lists the current choices of guidance algorithms to be used through each phase.

Table 1: Guidance Algorithms by Phase

Phase of Flight	Guidance Routine Option
Pre-SRM Coast	LVLH Hold – adjusts attitude to pre-determined LVLH pitch angle
	MEDeA – runs MEDeA descent algorithm, predicts starting LVLH pitch angle
SRM Burn	LVLH Hold – holds pre-determined LVLH pitch angle through duration of burn
	MEDeA – closed-loop SRM guidance for adjusting commanded LVLH pitch
Post-SRM Coast	Fixed time coast
Powered Decent	An Optimal Guidance Law for Planetary Landing[5]
	Augmented Apollo Powered Decent Guidance[6]
Vertical Alignment	Optional mode to pitch vehicle vertically
Vertical Decent	Linear velocity ramp-down, then linear position-velocity controller logic

In the Pre-SRM Coast phase, either a fixed known pitch angle relative to Local Vertical Local Horizontal (LVLH) frame is commanded, or a predicted required attitude at the start of the SRM burn is calculated and commanded by running the Moon Entry Descent Algorithm (MEDeA). In the SRM burn phase, again, either a fixed known LVLH pitch angle is commanded throughout the burn, or the MEDeA closed-loop guidance algorithm is executed and calculates the desired attitude. No guidance attitude is commanded in the Post-SRM Coast phase, and the vehicle is allowed to coast freely either using a fixed time or a time calculated by MEDeA.

The Moon Entry Descent Algorithm (MEDeA) is an integrated closed-loop guidance algorithm that accounts for the variations in the SRM thrust profile while staying within the liquid propellant budget. The SRM's thrust profile is estimated using curve fits of the projected hot, cold, and nominal temperature thrust profiles and an on-board calculated burn time. Using this estimated thrust profile, the SRM's pitch angle is adjusted during the descent using a numeric predictor-corrector method to achieve a pre-determined distance

from the desired landing site. At the end of the SRM burn and SRM disposal, a second predictor-corrector determines the minimum coast time needed for the vehicle to reach the desired landing site within the liquid propellant budget. The liquid thruster guidance is chosen by the trajectory designer to steer out state errors from the SRM burn and meet the mission constraints. For example, either a minimum acceleration guidance or the Apollo guidance could be used for the liquid portion.

The Moon Entry Decent Algorithm (MEDeA) is a predictor-corrector algorithm for the SRM burn. Internally, it simulates and predicts through all phases of flight to calculate a desired pitch angle in the LVLH frame. It uses an estimated thrust profile based on Propellant Mean Bulk Temperature (PMBT) to propagate the SRM phase of flight. The purpose of this algorithm is to ensure a good starting state for the Powered Decent phase. In the Powered Decent phase, two analytical algorithms are chosen from. The first algorithm, developed by D'Souza[5], is an optimal closed-loop feedback law which was analytically derived using the Euler-Lagrange equations, and assumes a linear acceleration profile. The second algorithm, Augmented Apollo Powered Decent Guidance (A2PDG[6]), is also analytical and allows for a wider range of acceleration and trajectory profiles.

An Optimal Guidance Law for Planetary Landing (D'Souza[5]), starts with Euler-Lagrange theory and solves an analytical expression for optimal control. The Cost index function is defined to minimize J given by following equation

$$J = \mathrm{T}t_f + \frac{1}{2}\int (a_x^2 + \dot{a_y^2} + a_z^2)$$

Which is subjected to:

$$\dot{\vec{r}} = \vec{v}$$
$$\dot{\vec{v}} = \vec{a} - \vec{g}.$$

Where T is a constant gain and t_f is the final time. a_x, a_y and a_z are components of acceleration expressed in the landing site frame. $\vec{r}$ and $\vec{v}$ are position and velocity, respectively. For the above problem, the flat earth assumption is applicable and $\vec{g}$, the gravity vector, is constant. If the objective is to target a final state $\vec{r}_f$ and $\overrightarrow{v_f}$, a linear form of analytical control is found given be following equation:

$$\vec{a} = -\frac{4}{t_{go}}\vec{v} - \frac{6}{tgo^2}\vec{r} - \vec{g}$$

In the above equation, t_{go} is the difference between current and the final time. t_{go} can be found by solving the following quartic equation, as referenced in D'Souza:

$$\left(\mathrm{T} + \frac{g_z^2}{2}\right)t_{go}^4 - 2\vec{v}\cdot\vec{v}t_{go}^2 - 12\vec{v}\cdot\vec{r} - t_{go} - 18\vec{r}\cdot\vec{r} = 0$$

A2PDG, developed by Ping Lu[6], assumes that the acceleration over the course of the burn takes the form of a quadratic, which is not necessarily optimal but adds an additional degree of control and is near optimal. For example, with D'Souza, a linear form of control allows control of the final position and final velocity. However, a quadratic form of control enables the control of the final acceleration as well. This feature is useful to control the orientation of the lander at the end of the Powered Descent phase. If the acceleration vector is constrained to align vertically to the landing site, then there is no need for a vertical alignment phase at the end of Powered Descent flight. Ping Lu presents A2PDG in his paper and gives an analytical closed-loop form for thrust direction and magnitude as follows:

$$a_T = \frac{2}{t_{go}}\left(1 - \frac{1}{3}k_r\right)\left[\vec{v}_f - \vec{v}\right] + \frac{k_r}{t_{go}^2}\left[\vec{r}_f - \vec{r} - \vec{v}t_{go}\right] + \left(\frac{1}{6}k_r - 1\right)\vec{a}_f + \left(\frac{1}{6}k_r - 2\right)\vec{g}$$

Guidance Performance

Figure 2 (L) below shows two 30-case Monte Carlo simulations that were ran to display the difference of landing positions from running D'Souza's optimal landing guidance and A2PDG, including navigation errors and state dispersions. As shown, both algorithms were accurately able to handle aligning the vehicle

vertically with the landing site well within the landing requirements. Data from the same two 30-case Monte Carlos is presented below in Figure 2 (R), which shows the trajectory profiles during Powered Descent guidance for all cases, including Navigation errors and state dispersions. In all cases, MEDeA is capable of ensuring that the vehicle is in a state at the end of the SRM burn that can be appropriately handled by both Powered Descent algorithms.

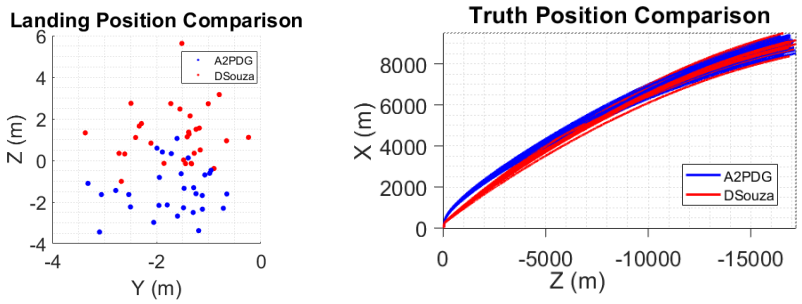

Figure 2: Landing Accuracy Comparison (L), As-flown Trajectory with Navigation Dispersions (R)

NAVIGATION SYSTEM DESIGN

The lander's Guidance architecture requires highly accurate knowledge of the vehicle's state during the entire descent mission in order to feed closed-loop guidance algorithms and enable landing within the requirements. As shown above in the flowdown of requirements, the vehicle must be able to land within 100m of a chosen landing site. The guidance algorithms outlined above are highly susceptible to navigation, as defined here to be knowledge, errors. Any incorrectness in the knowledge of position and velocity will directly add to the errors shown in the previous section to increase the uncertainty at landing. In order to meet the landing requirements, a robust set of sensors is required to support inertial navigation during descent. A baseline configuration was selected in order to provide external measurements to reduce navigation errors. These sensors are especially important due to constraints in terms of both weight and costs that limit the grade of inertial instrument possible. This baseline suite of sensors is described in the following sections, providing a summary of their operational characteristics, approach to integration and filtering, as well as integrated performance.

The external sensors limit the amount of navigation error due to inertial integration-induced errors. Correspondingly, the performance of the inertial sensors themselves drive the accuracy and operational requirements for the external sensors in order to meet final accuracy due to the lack of external measurements during the final period of flight at low altitudes. At these heights, the generation of dust and other effects due to ground-surface plume interaction may reduce the ability to operate. Due to these uncertainties, the systems are assumed to not have any external measurements upon final vertical descent. The effect of this constraint will be described in the following sections in the trades between various sensor requirements and integrated design, particularly in the area of vertical velocity knowledge at touchdown.

Baseline Sensor Suite

The integrated sensor package includes a variety of sensors enabling high accuracy knowledge of position and velocity during the descent. At the heart of the navigation system is an IMU, with requirements on par with the LN200S[*]. This IMU was chosen due to the team's prior experience with the unit on multiple terrestrial platforms[7] and its balance of SWAP, cost, and performance. While this sensor is capable enough to adequately support controls requirements in terms of rate and acceleration knowledge, the uncertainties from pure integration navigation are beyond the landing requirements. As such, additional sensors are used to augment the raw inertial measurements. An overview of the sensor suite is provided in Table 1. This suite is used to provide measurements of position and velocity to reduce knowledge errors. The primary aiding source to reduce state errors come from the use of TRN. While this technology has been operationally flown on

[*] https://www.northropgrumman.com/Capabilities/LN200FOG/Documents/ln200s.pdf

terrestrial vehicles[2] and is in development to support future Mars Missions[8 9], this will be one of the first operational applications of this technology in an extraplanetary landing mission. TRN operates by comparing an in-flight image of the planetary surface to a preloaded map. Through the use of computer vision algorithms, the sensor is able to provide an estimate of a planet-relative position. This accuracy is limited by the fidelity of the onboard map, processing capability, and imaging and lighting characteristics. At this stage of vehicle design, the project is focusing on position measurement accuracy requirements to define the TRN subsystem.

Table 2. Navigation Sensor Suite.

Sensor	Measurement	Operational Constraints
LN200S	High Rate Inertial Acceleration and Angular Rate	Entire Mission
Terrain Relative Navigation	Low Rate Inertial Position	Max Altitude and Min Altitude Constraints
Navigation Doppler LIDAR	High Accuracy 3-D Ranging and Velocity Relative to Surface	4000m to 30m
Star Tracker	Inertial Attitude Measurements	Cruise, up to SRM
DSN Update	Time, Inertial Position and Velocity	Cruise, prior to SRM

While this system does vastly improve translational position knowledge, it does have a limitation in the vertical axis and is coupled with the inherent instability in the vertical axis due to the effect of gravity errors. To provide additional knowledge in the vertical axis and provide a direct velocity measurement to the sensor integration suite, the use of NDL[2] has been baselined. This system provides a high accuracy measurement of both altitude and velocity via the use of multiple laser tracking heads.

One of the primary drivers of the landing performance is the initial uncertainty in terms of position, velocity, and attitude. Additional, onboard systems help to limit the initial errors prior to descent. The landing vehicle utilizes a star tracker to maintain a high accuracy attitude solution. This sensor will be used during the initial descent to constrain attitude errors. Similarly, the vehicle utilizes the DSN to provide a time, position, and velocity update prior to entering the descent maneuvers. Figure 3 defines the sensor availability during flight.

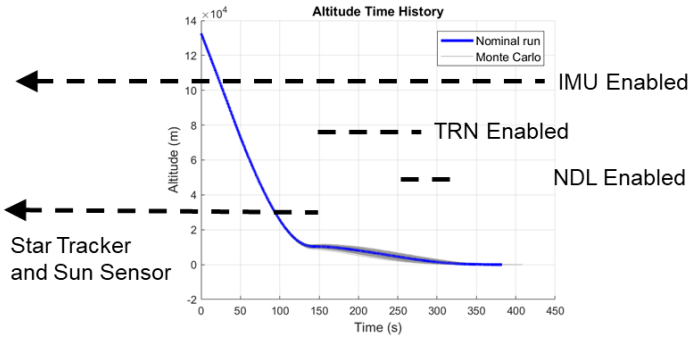

Figure 3: Sensor Operational Timeline

The onboard inertial integration algorithms utilize a simple 1st order Euler integration routine operating at 100 Hz. In order to simplify integration and operational transitions, the system utilizes separate attitude and state estimation filters. While not optimal and limits the ability of external measurements to influence the attitude state, this integrated attitude states have been shown to be within requirements for mission needs. Additionally, the attitude filter is a carryover from that used during the cruise stage of flight and allows for a stable transition to descent flight. An Extended Kalman Filter is used to provide updates to the integrated

position and velocity over the descent flight. The filter states include position error, velocity error, and accelerometer bias terms. This filter is initialized with uncertainty based on the last DSN update. De-coupling this filter from attitude states serves to simplify the filter, reducing numerical and computational complexity, while still allowing improvements to the onboard estimated states. Similarly, this system assumes a fully contained TRN sub-system, independent of the primary navigation algorithms that provides a position measurement. This does provide risk in terms of cascading filters, but the simulation responses demonstrate its capability within requirements and allows for the better defined subsystem boundaries easing systems integration. The flow of data between the systems is shown in Figure 4.

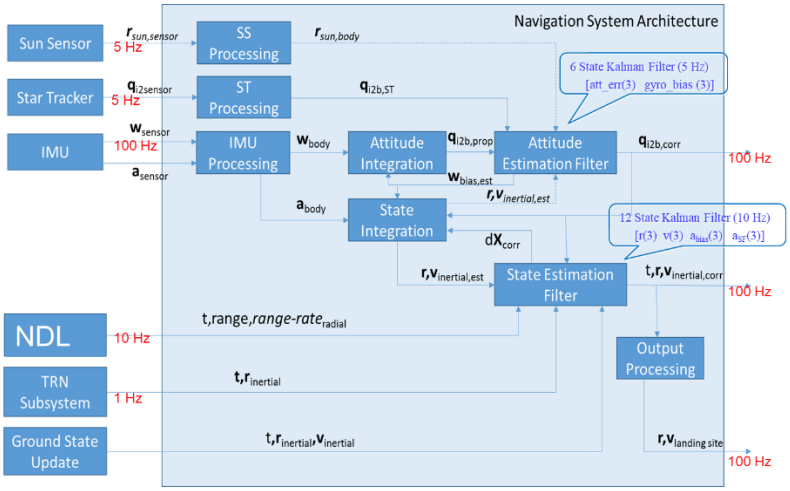

Figure 4: Navigation Architecture

In order to perform system estimation, the individual sensors are all modeled within the 6-Degree of Freedom (DOF) simulation framework. This framework utilizes error models specific to each sensor to capture the primary sensitivities. For the inertial navigation sensor, baseline errors such as bias, scale factor, noise, random walk, inter-sensor misalignments, and non-orthogonalities are captured. The star tracker error model has heritage to pervious programs utilizing similar hardware modeling attitude error independently about sensor roll and pitch-yaw axes. The TRN system is currently modeled as a sensor providing an inertial state estimate with errors captured in terms of position accuracy. The radar altimeter is modeled as lunar-centric velocity and altitude with errors focused on measurement precision, uncertainty, and mounting misalignment. This is necessary to capture the effect of attitude error coupling through the rotation of body-frame measurements into the inertial frame for use in the navigation algorithms. Modeling these errors within this framework allows for both covariance and statistical Monte Carlo-based analysis of the navigation system capabilities. This analysis capability also enables understanding of system sensitivities and requirements developments.

NAVIGATION SENSOR TRADES

One of the primary goals at this stage of development is to provide analysis to support subsystems definitions and requirements in order to develop interfaces and hardware elements. As such, a series of trades have been performed to provide insight into the sensitivities of the system to particular design attributes. This is particularly important in areas that will affect the vehicle's structural design, for example, allowable alignment knowledge requirements between various sensors when integrating measurements in a common vehicle frame. A landing position knowledge trade was performed to optimize the TRN and altimeter requirements.

Sensor Mounting Alignment Requirement Development

In order to move forward with developing sensor alignment knowledge requirements for the structural subsystem, two sensor alignment error trades were conducted within a simulation framework. The purpose of the first was to develop alignment requirements for the IMU and Star Tracker, and the purpose of the second was to develop alignment requirements for the NDL. Both trades were conducted independently,

although future work should include analysis with all sensors having alignment knowledge errors. A Monte Carlo approach was taken to analyze the effects of sensor alignment errors on Navigation error trends with respect to time and flight phase. Navigation errors at touchdown were compared to touchdown knowledge requirements. Each Monte Carlo was conducted using a Navigation stand-alone simulation, which utilized a fixed truth trajectory and was without Guidance and Control systems in the loop.

The first trade, which looked at the effects of IMU and Star Tracker alignment errors, consisted of 20 total 200 run Monte Carlos, sweeping across a range of 1-sigma IMU and Star Tracker misalignment angle statistics. Figure 5 below shows results for parameters most affected by these misalignments.

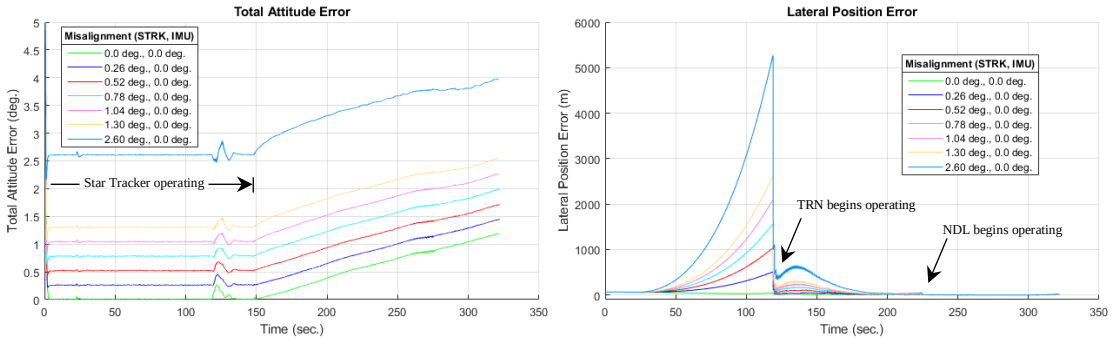

Figure 5: Star Tracker Misalignment Sensitivity

The time history plots show total attitude and lateral position errors as a function of time for a selection of runs from the Monte Carlos. Star tracker alignment errors translate directly to minimum attitude errors. After the star tracker turns off, attitude errors grow due to inertial navigation errors. The lateral position time history shows how inertial integration errors grow from the time of initialization to the point where TRN measurements become available. At certain sensor misalignment values, these errors grow to values on the order of 1000's of meters. Note that current lander guidance algorithms do not utilize lateral position knowledge during the pre-TRN phase of flight. However, lateral errors after the de-orbit burn finishes and TRN is available remain high for some misalignment angles. Touchdown attitude, position, and velocity errors were within requirements for 1-sigma angular alignment errors up to 1 deg. for the IMU and 1.5 deg. for the Star Tracker. This, however, does not indicate whether the guidance system will be capable of handling the navigation errors seen prior to touchdown. Lateral velocity errors were the touchdown navigation errors most influenced by star tracker and IMU misalignments.

The second trade, which looked at the effects of mounting alignment knowledge errors for the NDL, consisted of nine total 200 run Monte Carlos, sweeping across a range of 1-sigma NDL misalignment angle statistics. Figure 6 below shows results for parameters most affected by NDL misalignments.

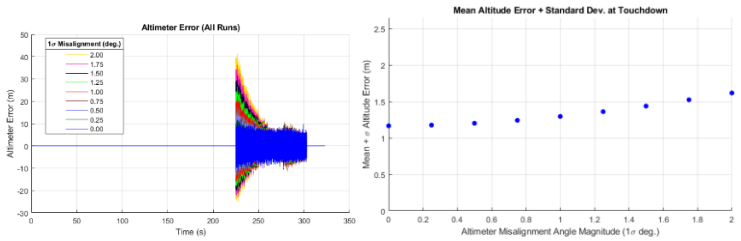

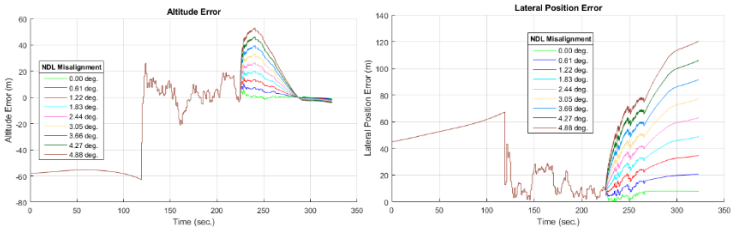

Figure 6: NDL Misalignment Sensitivity

The top left time history of Figure 6 is a carpet plot (9 x 200 runs) of altitude errors taken directly from the NDL planet model, prior to entering the Kalman Filter. Errors are plotted as zeroes at altitudes where the NDL is not operating. From Figure 6, it can be seen that altitude errors are larger for higher altitudes. Another thing to notice is that around 265 seconds into the simulation, altitude errors reduce to the noise level before expanding again. This occurs because at 265 seconds, the spacecraft's attitude is such that the NDL boresight vector (30 deg. tilted from the body vertical axis) is pointing directly down towards the lunar surface. After 265 seconds, the spacecraft rotates to its vertical descent attitude, meaning that the NDL boresight vector points 30 deg. off the vertical. These details show that raw NDL altitude errors are highly dependent on spacecraft altitude and attitude. It can be seen in Figure 6 that position errors increase predictably as NDL misalignment increases. Position errors plotted in the bottom row of Figure 6 represent the worst case runs from the nine Monte Carlos. While the lateral position knowledge meets navigation requirements for 1-sigma misalignment angles up to 1.5 deg., note that the altitude error is above 0.5 meters for all values of misalignment, even zero. No explicit altitude error requirement exists, but it has been stated that 0.5 m or less should be strived for. Altitude error must be below this value around touchdown to ensure that descent engine shutoff does not occur too early or too late. Potential solutions to the problem of excessive altitude errors at touchdown will be discussed later in this paper.

The two sensor alignment studies discussed above give insight into the requirements that will be leveraged on the structural subsystem. They will be used to inform future work, including running Monte Carlos with all sensors having alignment knowledge uncertainties, not just one or two at a time. Sensor alignment error requirements will be rolled into the full GLASS simulation for the lander for verification.

Landing Position Knowledge Sensor Requirement Trades

The primary driver of final lateral position knowledge is from the TRN sub-system. While the development and integration of the specific algorithms and sensors are still being traded, the simulation environment is ideal to identify performance and operational requirements. Even though the baseline assumptions on input parameters did demonstrate feasibility of meeting the mission goals, it is important to understand the robustness of the system. This also supports identifying the allowable margin in the requirements and supports risk assessments. In order to provide more insight into the system, the operational and performance constraints were relaxed to understand at what level the vehicle fails to meet landing knowledge. This information is key to identifying potential TRN solutions and allow tradability between subsystem performance and risk posture of the overall mission. With this information, trades can be made between schedule and cost with understanding of the incurred performance risk.

For this trade, a large 3000 case Monte Carlo was performed varying the key metrics of the TRN systems: minimal operational altitude, errors in estimated position, and update rate. The other sensors were dispersed as typical with their baseline performance metrics in order to focus on the integration of TRN with the other systems as-is. For each of the runs, a uniform distribution was used to select the performance and operation within the given range. A multivariate contour plot of the results is shown below in Figure 7. The results of were binned based on the two input variables values in the plot along the x- and y-axis (for each combination of variables). For the cases within the bin, the mean and standard deviation were computed. Finally, the mean is added to 3 times the standard deviation in order to capture the 99.73% probability of meeting the requirement. Using this value, the contour is then plotted showing the landing knowledge performance. The coloring of the contours is limited on the upper bound to 100 (the desired value). As such, anywhere in the space that is not yellow is a feasible design selection for the TRN system. From the plots, the low sensitivity between time between measurements and minimum altitude is shown. Essentially, as long as the measurement come

in at a high rate (less than 20 seconds), the minimum altitude (within that modeled) has little effect. This ensures the algorithm has adequate time with frequent measurement updates to reduce the state errors prior to the minimum altitudes. The sensitivity between min altitude and measurement performance is also clear. The better the measurement, the less sensitive the system is to when the outage occurs. Finally, a strong relationship can be seen between TRN measurement error and time between measurements. For example, as the error on a measurement goes up, a larger number of samples is needed to reduce the navigation uncertainty to be within the requirement. Conversely, if very accurate measurements are available, the time between them can be larger.

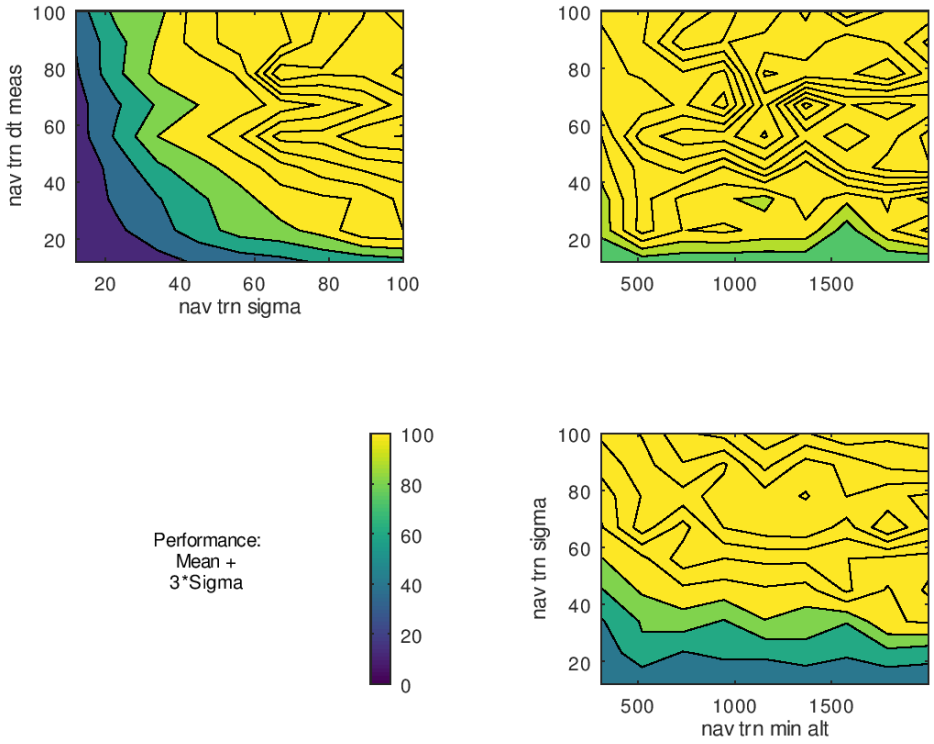

Figure 7: Multivariate of TRN Parameters

Together, these results can be used to set the broadest TRN metrics that will meet the mission. By applying constraints on each axis, it is possible to determine the area of feasibility. From the top right chart, 20 seconds is the largest time between measurements that met requirements regardless of altitude. The top left chart indicates that for this delay between measurements, the TRN error can be up to 100 m and still meet requirements. Applying these two insights to the lower right contours provides additional insight into the altitude constraint. To allow for largest minimum operational altitude, the error must be below 30m. And if allowing for the minimum altitude of 500m, the error can be as large as 60m. From this, the knowledge of the operational needs of the TRN system, principally the level of map fidelity, would drive the designer to allow for maximization of the minimal operating altitude to limit the required resolution of the map (for example, operation at lower altitudes would require a more detailed onboard map due to the limited size of the collected image). Similarly, this provides insight that as the TRN system matures, and the errors may increase beyond the initial requirement, the matching minimal operational altitude requirement can be updated to ensure mission success (in terms of navigation position knowledge).

Landing Velocity Knowledge-driven System Trades

Knowledge of the landing velocity is particularly important in order to ensure the vehicle's structure can survive touchdown. The velocity and altitude knowledge is used to turn off the lander's descent engines and

begin a drop to the surface. If commanded too soon, the vehicle may land with excess velocity that can damage the lander. Commanding shutdown too late causes additional interaction with lunar surface, potentially damaging any payload and the lander. Navigation altitude errors less than 0.5 m and navigation velocity errors close to zero are needed to ensure that the descent engines shut off at the correct time. The current navigation system performance is shown in Figure 8. The velocity error is acceptable, but the altitude error is not.

Two distinct phases of the lunar landing are highlighted as contributing to navigation errors at touchdown. The first is the phase where the NDL is available, which ends at 30 m altitude. The second is the phase where the lander navigates inertially from a 30 m altitude to descent engine shutoff. NDL is not trusted below a 30 m altitude since that is where it is assumed that substrate from the lunar surface starts being kicked up. A dedicated low altitude altimeter is proposed to mitigate altitude errors prior to the 30 m NDL shutoff. Processing the NDL sensor signal requires knowledge of sensor orientation relative to an inertial frame, meaning that spacecraft attitude is required for the calculation. It was found via Monte Carlo that attitude errors become high enough by the time NDL reaches its final measurements that the processed altitude measurement from the sensor has an error above 0.5 m (even with noise removed). One option is the inclusion of a dedicated low-altitude altimeter for additional and better quality altitude measurements just prior to NDL shutoff.

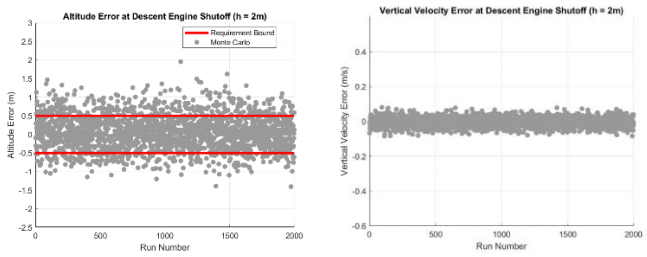

Figure 8: Nominal Navigation Performance at Descent Engine Shutoff

It was assumed that the dedicated low-altitude altimeter would output measurements at 10 Hz in two short 1 second bursts while descent engines were momentarily turned off. These two bursts were assumed to begin at altitudes of 100 m and 50 m, respectively. Measurement noise was assumed to be 0.1 m 1-sigma. The dedicated altimeter was assumed to be pointing along the spacecraft vertical axis towards the Moon. A 2,000 run Monte Carlo was conducted to analyze the altitude knowledge improvements provided by the inclusion of the dedicated low-altitude altimeter. The results of this study are shown in Figure 9.

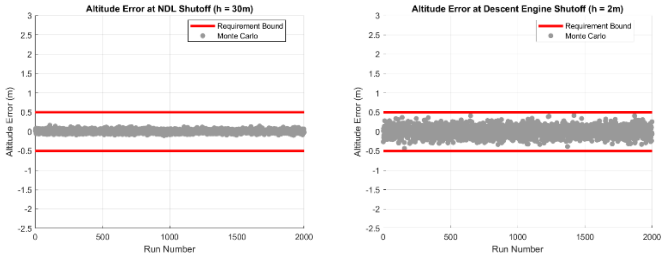

Figure 9: Navigation Altitude Performance with Dedicated Altimeter

By comparing the two plots in Figure 9, the effect of integrating for the final 30 m of descent without external measurements can be seen. Because this inertial integration of IMU accelerations pushes the navigation errors close to the requirement boundary, accurate accelerometer bias estimation within the filter will need to be matured or implemented during the coast period prior to descent. From these results, it is recommended that the dedicated low altitude altimeter be added to the sensor suite and the feasibility of a period of accelerometer bias estimation be further examined. Two other potential changes to the lander may impact the recommendations of this study. First, a higher performance IMU may be chosen. This has been shown to reduce Navigation errors at descent engine shutoff both by reducing inertial drift and reducing attitude errors

when the NDL is active. Second, physical touchdown sensors, like those used for the Apollo lunar lander, are being explored by the structural subsystem. If they are implemented, physical sensors would negate the need for sub-0.5 m altitude knowledge at descent engine shutoff.

CONCLUSIONS AND FUTURE WORK

This paper provides a summary of the primary guidance and navigation trades performed in support of the Lunar Pallet Lander project. The current design is able to demonstrate feasibility of using existing and in-development sensors to enable high precision landing of large payloads to the Lunar surface. As the vehicle continues to move forward on the path towards flight, these trades will continue to be matured and drive vehicle specifications and subsystem requirements. In addition to the current application, these technologies will form the basis of any human mission and lay the groundwork for precise deployment and landing of extensive planetary resources. Similarly, the results of these algorithms demonstrate the feasibility of high accuracy landing applications. These results are enabled by the maturity of the sensor and vehicle models, allowing for the team to perform extensive, in-depth analysis of full vehicle simulation, allowing for insight and understanding of the complex interactions between all flight systems. This early insight into GNC capability is necessary to ensure adequate sensor selection and algorithm development needed to support the mission's capabilities. With the continued development of this vehicle, these technologies will continue to be demonstrated, proven, and exercised in future missions.

ACKNOWLEDGMENTS

The team would like to acknowledge the support of the Lunar Pallet Lander project in supporting this work and publication. Additionally, we would like to express our gratitude for the support of our branch and division management in their continued support of small project and technology development missions.

REFERENCES

[1] Johnson, Andrew E., and James F. Montgomery. "Overview of terrain relative navigation approaches for precise lunar landing." 2008 IEEE Aerospace Conference. IEEE, 2008.

[2] Pierrottet, Diego, et al. "Navigation Doppler Lidar sensor for precision altitude and vector velocity measurements: flight test results." Sensors and Systems for Space Applications IV. Vol. 8044. International Society for Optics and Photonics, 2011.

[3]Orphee, Juan, et al. "Guidance, Navigation, and Control for NASA Lunar Pallet Lander." *Proceedings of the AAS Guidance and Control Conference*, Breckenridge, CO., 2019.

[4] Ronald Sostaric and Jeremy Rea. "Powered Descent Guidance Methods For The Moon and Mars", AIAA Guidance, Navigation, and Control Conference and Exhibit, Guidance, Navigation, and Control and Co-located Conferences, 2005.

[5] D'Souza, Christopher. "An optimal guidance law for planetary landing." AIAA Guidance, Navigation, and Control Conference. 1997.

[6] Lu, Ping. "Augmented Apollo Powered Descent Guidance." Journal of Guidance, Control, and Dynamics, AIAA, 2018.

[7] McGee, Timothy G., et al. "Mighty Eagle: The Development and Flight Testing of an Autonomous Robotic Lander Test Bed." Johns Hopkins APL Technical Digest 32.3 (2013): 619-635.

[8] Johnson, Andrew E., et al. "Design and analysis of map relative localization for access to hazardous landing sites on mars." AIAA Guidance, Navigation, and Control Conference. 2016.

[9] Johnson, Andrew E., et al. "Real-time terrain relative navigation test results from a relevant environment for Mars landing." AIAA Guidance, Navigation, and Control Conference. 2015.